

# Multi-Carrier (OFDM) Cooperative Transmission in MANETs with Multiple Carrier Frequency Offsets

Mus'ab Yüksel  
Hochschule Darmstadt  
Darmstadt, Germany  
musab.yueksel@h-da.de

Raphael T. L. Rolny  
armasuisse Science and Technology  
Thun, Switzerland  
raphael.rolny@armasuisse.ch

Marc Kuhn  
ZHAW  
Winterthur, Switzerland  
kumn@zhaw.ch

Michael Kuhn  
Hochschule Darmstadt  
Darmstadt, Germany  
michael.kuhn@h-da.de

**Abstract**—Cooperative transmission, realized by aggregating several nodes to a virtual multiple input system, is an auspicious approach to establish a more robust and effective communication in MANETs. In such a setup, impairments, i. e. multiple timing and carrier frequency offsets (TO, CFO) will occur. While multi-carrier schemes, e. g. Orthogonal Frequency Division Multiplexing (OFDM), are well-known to mitigate the impact of multipath propagation and TO, multiple CFO causes inter-carrier-interference (ICI) which typically degrades the performance significantly. Within this paper, we propose an effective code and equalizer structure that allows to overcome this limitation. It mitigates the impact of multiple CFO that can be significantly larger than the subcarrier spacing with a reasonable computational effort. For that, we utilize inherent code properties of Linear-Scalable Dispersion Codes (LSDCs) and propose a communication system composed of an equalizer structure in combination with LSDCs that enables multi-carrier distributed cooperative transmission for practical MANETs with high node mobility. We demonstrate the benefits of cooperative transmission in comparison to classical non-cooperative multi-hop or concurrent transmission by outage simulations, which clearly indicate that our proposal can be of crucial importance for the overall MANET scalability. Lastly, we compare our OFDM system with a recently proposed time-domain equalization single-carrier system and point out use cases, where the OFDM system can be more advantageous.

**Index Terms**—MANET Scalability, Distributed Cooperative Transmission (Broadcasting), Space-Time Block Codes (STBC), Carrier Frequency Offset (CFO), Timing Offset (TO), OFDM

## I. CRITICALITY OF CARRIER FREQUENCY OFFSET

Mobile Ad-Hoc Networks (MANETs) do not require any infrastructure and are typically composed of lightweight, low-power, low-cost nodes [1]. Cooperative transmission can be established by aggregating several nodes to a virtual multiple input system. If a transmit diversity scheme is employed, all nodes simultaneously send the same information, but a different transmit signal, so that the contributions add up in power and not in amplitude. By that, destructive interference can be avoided [2].

With respect to practical systems several impairments have to be considered as depicted in Fig. 1, that particularly arise due to the aggregation of distributed nodes. As all nodes are located at a different distance to each other, the propagation time varies leading to a timing offset (TO). Imperfect synchronization will also cause TO. Besides, multipath propagation has to be expected that causes a channel delay spread which

is dissimilar for each link. Since each node is equipped with an own oscillator, in principal each will induce a different carrier frequency offset (CFO), while node mobility is a further source for CFO due to the Doppler shift. The latter is specifically an issue for the increasingly popular Vehicular or Flying Ad-Hoc Networks (VANETs [3], FANETs [4]).

Multi-carrier modulation schemes, like Orthogonal Frequency

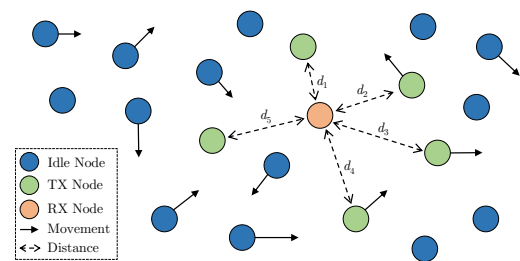


Fig. 1. MANET system model: distributed nodes each with a different oscillator, moving direction, velocity and distance to other nodes

Division Multiplexing (OFDM), are commonly known to be suited to overcome multiple TO and multipath propagation by an appropriately designed guard interval, i. e. cyclic prefix. However, they greatly suffer from the impact of multiple CFO that causes inter-carrier-interference (ICI). In literature, two different approaches are followed to deal with this problem. On the one hand, transmit diversity schemes are proposed that are insensitive to CFO. However, these typically cannot achieve full transmit diversity and rate one simultaneously [5]. On the other hand, mitigation techniques are proposed. Nonetheless, these have major drawbacks. The performance can often only be maintained if the CFO is comparably low [5], [6] or significantly increased computational effort is required [7]. Some mitigation techniques require an extended overhead [8] or are limited to a specific, rather low number of transmitters [7], [9].

Within this paper, we propose an effective equalizer structure which facilitates cooperative communication that

- is insensitive to arbitrary multiple CFO,
- is robust against multiple TO,
- profits from multipath propagation,
- allows for an arbitrary number of TX,
- is computationally efficient and

- does not require any additional overhead, knowledge about the nodes' location or a feedback link.

We employ Linear-Scalable Dispersion Codes (LSDCs) [10] as transmit diversity scheme and utilize inherent code properties. In Section V, we demonstrate the effectiveness of the proposed equalizer structure and cooperative transmission by investigating the propagation of a message in a MANET scenario. Lastly, we compare our OFDM system with a recently proposed time-domain equalization single-carrier system [11]. *Notation:*  $x$  denotes a scalar,  $\mathbf{x}$  a vector,  $\mathbf{X}$  a matrix and  $\ddot{\mathbf{X}}$  a diagonal matrix where  $\mathbf{X}(i, j) = 0$  for  $i \neq j$ .  $(\cdot)^H$  refers to the adjoint (complex transpose),  $(\cdot)^\Omega$  to a frequency domain and  $(\cdot)_i$  to a node specific description.

## II. TRANSMIT DIVERSITY SCHEME

Space-Time Block-Codes, initially designed for co-located antennas at one node, can be adapted to establish cooperative transmission for distributed nodes [2]. It could be shown, that LSDCs are a favourable option as they rely on an artificially introduced interference to achieve the best-possible diversity performance [2]. Fundamentally, two linear codes are used for encoding. The outer code  $\mathbf{R} \in \mathbb{C}^{N_C, N_I}$  is optimized with respect to the diversity gain, while the inner code  $\mathbf{C}_\nu \in \mathbb{C}^{N_C, N_{TX}}$  is designed for channel adaptation, where  $N_C$  denotes the block length,  $N_I$  the number of information symbols and  $N_{TX}$  the number of transmitters (TX). According to [10] the matched received symbol vector  $\mathbf{y}_m \in \mathbb{C}^{N_C, 1}$  is obtained by

$$\mathbf{y}_m = \mathbf{R}^H \cdot \ddot{\mathbf{D}} \cdot \mathbf{R} \cdot \boldsymbol{\alpha} + \mathbf{n} = \boldsymbol{\Lambda} \cdot \boldsymbol{\alpha} + \mathbf{n}, \quad (1)$$

where  $\mathbf{n} \in \mathcal{CN}(0, \sigma_n^2 \mathbf{I})$  denotes the complex-valued additive white Gaussian noise (AWGN).  $\ddot{\mathbf{D}} \in \mathbb{C}^{N_C, N_C}$  is a diagonal matrix that summarizes the impact of the channel and the inner code. In [12] an OFDM design is proposed that basically uses the exact same encoding approach as for a single-carrier scheme. However, this is only possible for a co-located setup, i. e. in absence of multiple CFO.

### A. OFDM Encoding for Distributed Nodes

Applying a transmit diversity scheme for OFDM basically allows to profit from several degrees of freedom. If all subcarriers are considered as one block, the frequency selectivity of the channel can be utilized, so that *diversity over frequency* can be attained. Besides, *diversity over space* can be achieved if several nodes are aggregated to a cooperative transmission. Additionally, it is possible to accomplish *diversity over time* if different OFDM symbols are accumulated and if various observations for the same OFDM subcarrier are considered as one block. In principle, all mentioned diversity gains can be hit simultaneously. Nonetheless, a sufficiently large block-length is necessary that in turn increases the decoding complexity. Within this paper we will focus on an encoding that facilitates diversity over frequency and space.

The transmit symbol vector  $\boldsymbol{\alpha}_{TX} \in \mathbb{C}^{N_C, 1}$  is generated by  $\boldsymbol{\alpha}_{TX} = \mathbf{R} \cdot \boldsymbol{\alpha}$ , where  $\boldsymbol{\alpha} \in \mathbb{C}^{N_C, 1}$  denotes the input (information) symbol vector. Thereafter, each node  $i$  uses a different inner code  $\ddot{\mathbf{C}}_{TX,i}$  to calculate its specific transmit symbol vector.

$\ddot{\mathbf{C}}_{TX,i}$  is a diagonal matrix whose elements correspond to one column of the inner code matrix  $\mathbf{C}_\nu$ . In order to obtain the specific OFDM symbols  $\boldsymbol{\beta}_{TX,i}$ , in general guard and pilot carriers are adjoined according to the OFDM design. Next, the time-domain transmit symbol is generated by performing a  $N_{sc}$ -point IDFT which can be expressed by employing a DFT-matrix  $\mathbf{F} \in \mathbb{C}^{N_{sc}, N_{sc}}$  as  $\tilde{\mathbf{u}}_i = \sqrt{\frac{1}{N_{sc}}} \cdot \mathbf{F}^H \cdot \boldsymbol{\beta}_{TX,i}$ . Lastly, a cyclic prefix of length  $L_{cp}$  is added by prepending the last  $L_{cp}$  samples to obtain the transmit signal  $\mathbf{u}_i$  for the  $i$ -th TX.

### B. Impact of CFO

Basically, a different multipath fading channel for the link between each TX and RX is assumed (tapped delay line modelling, broadband channel in the time-domain), while the channel for one OFDM symbol and the  $i$ -th link can be described by a channel vector  $\mathbf{h}_i \in \mathbb{C}^{N_{sc}, 1}$  that can be expressed as  $\mathbf{h}_i = (h_{i,1} \ h_{i,2} \ \dots \ h_{i,L_{cp}} \ 0 \ \dots \ 0)^T$ . The number of non-zero channel coefficients, i. e. the number of paths (channel taps), is assumed to be not larger than the cyclic prefix length to maintain orthogonality of the OFDM subcarriers. In the time-domain, the impact of the channel can be expressed by a linear convolution as  $\mathbf{u}_{ch,i} = \mathbf{h}_i * \mathbf{u}_i$  or respectively as  $\mathbf{u}_{ch,i} = \mathbf{h}_i * \mathbf{u}_i + \mathbf{n}$ .

We assume that the CFO is different for each TX and constant for at least one OFDM block. As CFO results from the mismatch between the oscillators of each TX and RX, the impact in time-domain can be considered by a multiplication with a diagonal matrix  $\ddot{\Phi}_{TX,i}$  prior to the superposition of the intermediate signals  $\mathbf{u}_{ch,i}$ . The  $\nu$ -th diagonal element of  $\ddot{\Phi}_{TX,i}$  corresponding to the  $\nu$ -th time-slot can be expressed by

$$\ddot{\Phi}_{TX,i}(\nu, \nu) = e^{j \cdot 2\pi \cdot \text{CFO}_i \cdot \nu \cdot t_s} = \phi_i^\nu, \text{ so that} \quad (2)$$

$$\ddot{\Phi}_{TX,i} = \begin{pmatrix} \phi_i^0 & 0 & \dots & \dots & 0 \\ 0 & \phi_i^1 & 0 & \dots & 0 \\ \vdots & 0 & \ddots & 0 & 0 \\ \vdots & \vdots & \vdots & \ddots & 0 \\ 0 & 0 & 0 & 0 & \phi_i^{2 \cdot N_{sc} + L_{cp} - 2} \end{pmatrix}, \quad (3)$$

where  $\text{CFO}_i$  refers to the CFO of the  $i$ -th TX and  $t_s$  to the sample time of the system. With that, the received symbol vector  $\mathbf{y}$  can be denoted as

$$\mathbf{y} = \sum_{i=1}^{N_{TX}} \ddot{\Phi}_{TX,i} \cdot \mathbf{u}_{ch,i} = \sum_{i=1}^{N_{TX}} \ddot{\Phi}_{TX,i} \cdot (\mathbf{h}_i * \mathbf{u}_i + \mathbf{n}). \quad (4)$$

## III. PROPOSED EQUALIZER STRUCTURE

The procedure to obtain the proposed equalizer structure is similar to that in [11]. The overall transmission is summarized in the frequency domain by employing a correlation matrix  $\boldsymbol{\Lambda}$  that is in the form of

$$\boldsymbol{\Lambda} = \mathbf{R}^H \cdot \boldsymbol{\Lambda}_Q \cdot \mathbf{R}, \text{ so that} \quad (5)$$

$$\mathbf{y}_m = \boldsymbol{\Lambda} \cdot \boldsymbol{\alpha} + \mathbf{n} = \mathbf{R}^H \cdot \boldsymbol{\Lambda}_Q \cdot \mathbf{R} \cdot \boldsymbol{\alpha} + \mathbf{n}. \quad (6)$$

Once a matrix  $\Lambda_Q \in \mathbb{C}^{N_c, N_c}$  can be found that merges the impact of aforementioned impairments and at the same time fulfils equations (5) and (6),  $\mathbf{R}$  can be optimized to maximize the pairwise product distance [10]. So, a high diversity gain can be achieved, whereas the optimization depends on the structure of  $\Lambda_Q$ . The performance can be retained, once the additional ICI can be sophisticatedly considered. For that, inherent code properties of LSDCs are utilized, which highlights the proposal from [2].

To determine  $\Lambda_Q$ , we employ an intermediate matrix  $\mathbf{Q} \in \mathbb{C}^{N_c, N_c}$  that summarizes the transmit behaviour or respectively properties for all links.  $\mathbf{Q}$  can be obtained by a superposition of each links' property matrices  $\mathbf{Q}_{\text{TX},i} \in \mathbb{C}^{N_c, N_c}$ , so that  $\Lambda_Q = \mathbf{Q}^H \cdot \mathbf{Q}$ , whereas  $\mathbf{Q} = \sum_{i=1}^{N_{\text{TX}}} \mathbf{Q}_{\text{TX},i}$ . Crucial for the presented approach is to describe the impact of CFO in the frequency-domain. A matrix  $\Phi_{\text{TX},i}^\Omega$  that incorporates latter can be constructed by

$$\Phi_{\text{TX},i}^\Omega = \frac{1}{N_{\text{sc}}} \cdot \mathbf{F}^H \cdot \ddot{\Phi}_{\text{TX},i} \cdot \mathbf{F}. \quad (7)$$

It is noteworthy, that  $\Phi_{\text{TX},i}^\Omega$  is no diagonal matrix anymore, but a cyclic matrix. Hence, each subcarrier is interfering with all other subcarriers, whereas this ICI is the larger, the larger the CFO is. Using  $\Phi_{\text{TX},i}^\Omega$  for each TX,  $\mathbf{Q}_{\text{TX},i}$  can be built as

$$\mathbf{Q}_{\text{TX},i} = \Phi_{\text{TX},i}^\Omega \cdot \ddot{\mathbf{H}}_{\text{TX},i} \cdot \ddot{\mathbf{C}}_{\text{TX},i}, \quad (8)$$

where  $\ddot{\mathbf{H}}_{\text{TX},i}$  denotes the channel for the  $i$ -th link in frequency-domain that can be obtained by  $\ddot{\mathbf{H}}_{\text{TX},i} = \text{diag}(\mathbf{F} \cdot \mathbf{h}_i)$ .

For the processing at the RX, first the cyclic prefix of the received symbol vector is removed, before the frequency-domain expression is calculated by  $\mathbf{y}^\Omega = \sqrt{\frac{1}{N_{\text{sc}}}} \cdot \mathbf{F} \cdot \mathbf{y}$ .

Next, a multiplication with the adjoint transmit property matrix  $\mathbf{Q}^H$  is performed prior to a multiplication with the adjoint outer code matrix  $\mathbf{R}^H$ , so that  $\mathbf{y}_m$  is obtained by

$$\mathbf{y}_m = \mathbf{R}^H \cdot \mathbf{Q}^H \cdot \mathbf{y}^\Omega. \quad (9)$$

The corresponding correlation matrix  $\Lambda$  promptly follows as

$$\Lambda = \mathbf{R}^H \cdot \mathbf{Q}^H \cdot \mathbf{Q} \cdot \mathbf{R}. \quad (10)$$

$\mathbf{y}_m$  and  $\Lambda$  can be forwarded to an appropriate decoder (see Fig. 3). It is important to denote, that the proposed equalizer structure does not majorly increase the complexity with respect to the initial system, as the main properties of the correlation matrix  $\Lambda$  retain similar. Compared to the starting system, the composition of the  $\mathbf{Q}$  and  $\mathbf{Q}_{\text{TX}}$  matrices are an extra burden, which however is a set of simple matrix multiplication and addition operations. Thus, it can be considered easily feasible, even for less powerful computational devices. The overall complexity of the equalizer is in principle scalable by replacing the employed decoder. Linear decoder instead of an iterative MAP-MMSE-DFE can be also used, whereas it is on hand that there will be a performance degradation compared to iterative representatives due to the enhanced interference cancelling capability of latter. The MAP-MMSE-DFE receiver in particular allows for a complexity-performance trade-off by

adjusting the decision threshold.

The overall system model is summarized in the block diagram that is depicted in Fig. 2, presuming that the channel impulse response is not longer than the guard interval and that no oversampling is performed. Besides, Fig. 3 visualizes the proposed equalizer structure that considers multiple CFO which the initial design does not.

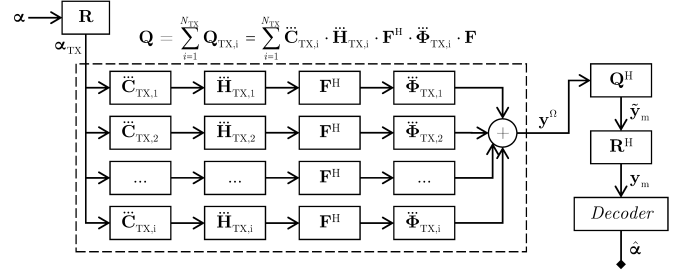


Fig. 2. Equivalent system model summary

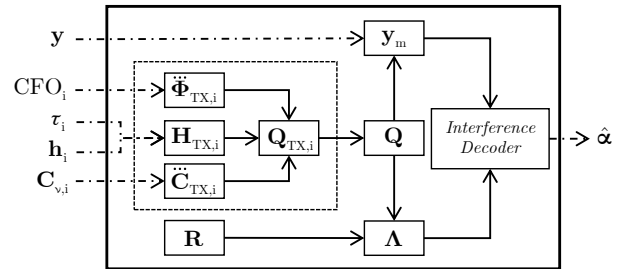


Fig. 3. Proposed equalizer structure that considers multiple CFO

#### IV. PERFORMANCE COMPARISON

Within this section we momentarily concentrate on a MANET setup with  $N_{\text{TX}} = 4$  transmitters to validate the robustness of our proposed equalizer structure prior to evaluating the propagation of a message in a larger more realistic MANET scenario in Section V. First, we define an exemplarily OFDM design in accordance to the requirements considered for the NATO Narrowband Waveform (NBWF) [13].

##### A. Environmental Conditions for NBWF

A maximum delay spread of  $\tau_{\text{max}} = 100 \mu\text{s}$  and a maximum node velocity of  $v = 60 \text{ kmh}^{-1}$  is presumed. Besides, the MANET is considered to be operated in the UHF frequency range, wherefore a carrier frequency of  $f_c = 500 \text{ MHz}$  is assumed. With these, the maximum Doppler frequency  $f_{\text{D,max}}$  follows as  $f_{\text{D,max}} = \frac{v}{c} \cdot f_c = 27.78 \text{ Hz}$ , the channel coherence time  $T_c$  as  $T_c < \frac{1}{2 \cdot f_{\text{D,max}}} = 18 \text{ ms}$  and the channel coherence bandwidth  $B_c$  as  $B_c < \frac{1}{2 \cdot \tau_{\text{max}}} = 5 \text{ kHz}$ .

##### B. Exemplarily OFDM Design

Aiming for a robust transmission, the cyclic prefix is chosen to be as long as the assumed maximum delay spread ( $T_{\text{cp}} = \tau_{\text{max}} = 100 \mu\text{s}$ ), which corresponds to a path length difference of  $\Delta d_{\text{cp}} = c_0 \cdot T_{\text{cp}} = 30 \text{ km}$ . The symbol duration is four times longer than the guard interval, so that  $T_{\text{sym}} = 4 \cdot T_{\text{cp}} = 400 \mu\text{s}$ .

Hence, the subcarrier spacing is  $\Delta f = \frac{1}{T_{\text{sym}}} = 2.5$  kHz. Aiming for a necessary bandwidth below 80 kHz according to NBWF and requiring  $N_{\text{SC}} \in 2^x, x \in \mathbb{N}$  for computational efficiency, we select  $N_{\text{SC}} = 32$ , so that  $B_{\text{OFDM}} = N_{\text{sc}} \cdot \Delta f = 80$  kHz and  $t_s = \frac{T_{\text{sym}}}{N_{\text{sc}}} = 12.5 \mu\text{s}$  for further proceeding. Then, the effective bit rate for 4-QAM is  $R_{b,\text{OFDM}} \approx 100$  kbps. It is important to denote, that the proposed equalizer structure is not limited to a 4-QAM. Employing higher order schemes is straightforward and only increases the computational complexity for decoding.

Due to the small coherence bandwidth in comparison to the subcarrier spacing, it appears to be less favourable to embed pilot carriers into each OFDM symbol. Instead, we presume that the parameters are estimated with training symbols. For the performed simulations, it is assumed that the RX has perfect knowledge about the channel state information as well as perfect knowledge about each TX' CFO and each link's delay. Such a precise parameter estimation is reasonable, as the feasibility of varying approaches has been demonstrated in theory [14] and with low-complexity SDRs [15].

With regard to the large coherence time in comparison to the symbol duration, it becomes apparent that aiming for diversity over time would be disadvantageous for such a setup.

Following typical OFDM designs, the DC-carrier is suppressed. Besides, left and right guard carriers are considered. In total 26 out of 32 carriers are used for data transmission.

### C. Results

We assume that each node introduces CFO and limit the simulations on oscillators with an accuracy of 100 ppm, so that the CFO is randomly varied between  $\pm 50$  kHz for each TX and transmission. Thereby, the overall received signal spectrum is considered to be totally covered by the filter bandwidth. We further presume Rayleigh fading channels (tapped delay line modelling) and vary the number of paths  $N_{\text{paths}}$  (channel taps), i. e. the distinctness of multipath propagation. A power-decay-profile is not considered, so that each path has the same mean power. Hence, each channel coefficient vector is scaled by  $\sqrt{\frac{1}{N_{\text{paths}}}}$ . For the moment, we do not consider any distance-dependent path-loss and assume that all TX are located at the approximately same distance to the RX, but the channel for each link is different. In addition, each link introduces a random TO, whereas  $\tau$  denotes the maximum delay in samples, so that the link specific delay  $\tau_i \in (0, \tau)$ . The overall delay (TO and channel delay spread) does not exceed the cyclic prefix.

With respect to the LSDCs, the outer code length is selected such, that  $N_C = N_{\text{data}}$ . The number of information symbols matches  $N_C$  ( $N_I = N_C = 26$ ), so that rate one is attained ( $R_C = \frac{N_I}{N_C} = 1$ ). A numerically optimized outer code is employed according to [10], while a random phase matrix is used as inner code [2]. An iterative MAP-MMSE-DFE receiver [16] is utilized, whereas the decoding error threshold is set to 0. So, only one symbol is decoded per iteration.

From Fig. 4 it becomes immediately clear, that the proposed equalizer structure is capable to retain the diversity perfor-

mance in presence of multiple TO and CFO. Multipath propagation cannot only be compensated, but is even advantageous, as the outer code is able to utilize the induced frequency selectivity. In fact, this has been a major reason for our preference for LSDCs in favour of other STBCs.

We compare our results with classical non-cooperative multi-

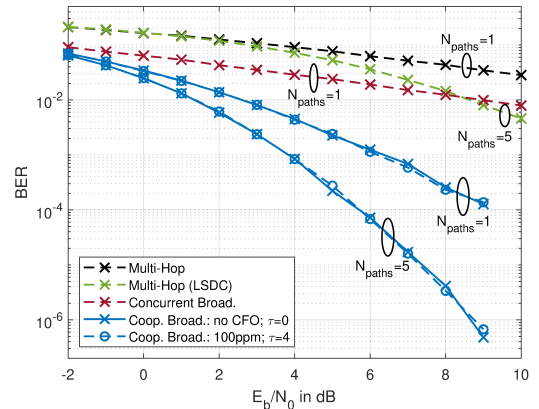


Fig. 4. Performance comparison: BER vs.  $\frac{E_b}{N_0}$  for classical multi-hop, concurrent and cooperative communication

hop communication where only 1 TX is active at a time [2]. It can be differentiated, whether the single TX employs LSDC encoding to achieve diversity over frequency. For latter, the same outer code can be utilized as for cooperative transmission, while the inner code has only one non-zero column. According to aforementioned observation, encoding a single node's signal with an appropriate outer code is advantageous in a multipath environment. Nonetheless, the performance that is achievable with a cooperative transmission is significantly better, particularly for small  $N_{\text{paths}}$ , as then the achievable diversity over space dominates the diversity over frequency. Besides, we compare our results with *concurrent* transmission [2]. In such a scenario, all active nodes indeed transmit simultaneously, but without using any transmit diversity. Because all TX accordingly send the same information and signal, destructive interference can occur that has a negative impact on the performance. Within this context, it is important to denote that our proposed equalizer structure directly allows to mitigate the impact of multiple CFO for concurrent transmission, too. The same model is valid, whereas the outer code is replaced by the identity matrix of appropriate dimension and  $\mathbf{C}_v$  is a matrix purely consisting of ones. Again, it has to be stated, that *cooperative* transmission is significantly more robust.

## V. MANET SIMULATIONS

Within this section we simulate the propagation of a message in a MANET that consists of a varying number of nodes ( $N_{\text{nodes}}$ ). We exemplarily study a cooperative broadcasting scenario that is perfectly suited to highlight the benefits of the proposed equalizer architecture: More and more nodes become active each introducing a varying CFO in the range  $\pm 50$  kHz, since we again assume 100ppm oscillators and  $f_c = 500$  kHz. At the beginning, one node starts to transmit a message.

Surrounding nodes that are able to successfully decode, join the transmission and become TX. All active TX send simultaneously, why an increased number of TX is employed for each broadcasting stage, so that the transmission range is typically extended and the number of required hops reduced [2].

To identify the broadcast success, we generate random topologies and study the propagation of a message stage by stage. For each stage, we simulate several channel realizations and calculate the mean BER for each receiving node. If the mean BER is below  $10^{-2}$  we consider the node to be reached, while we choose this threshold with respect to common forward error correction (FEC) schemes, that typically allow to correct remaining bit errors once this BER level is undercut. A stage is successful if at least one further node can be reached. Accordingly, a broadcast is successful if all nodes can successfully decode the message. The evaluation algorithm is condensed in Fig. 5.

For our simulations we assume that  $N_{\text{nodes}}$  are randomly

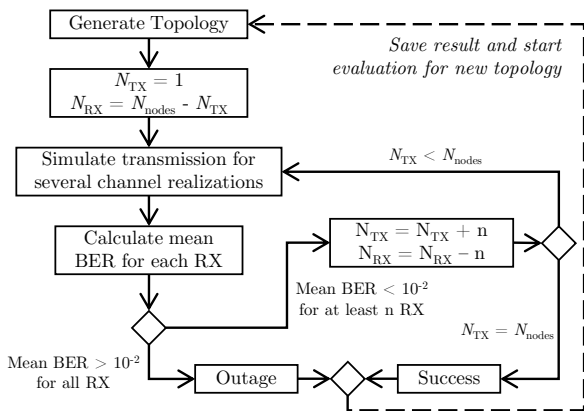


Fig. 5. Algorithm to detect outage / success in MANET simulations

distributed in a two-dimensional (all nodes are at the same height) area of dedicated size (10m x 10m). We assume Rayleigh fading channels for each link, which are different for each stage, and vary the number of paths. The channel coefficient vectors are scaled with  $\sqrt{d_i^{-\eta}}$ , where  $d_i$  refers to the distance between the  $i$ -th TX to the corresponding RX and  $\eta = 4$  to the path-loss coefficient of a suburban environment, to consider a distance-dependent path-loss. Each node introduces a random CFO, while the TO for the  $i$ -th link is also distance-dependent. It is determined by

$$\tau_i = \left\lceil 1 \frac{\text{sym}}{\text{m}} \cdot (d_i - d_{\min}) \right\rceil. \quad (11)$$

With Eq. 11 we map the distance of each TX to the respective receiving node to a corresponding propagation time. The difference between these is considered a TO. Thereby, we declare each TO with respect to the earliest arriving signal that is originated from the nearest located node, where  $d_{\min}$  refers to the minimum distance between all active TX to the RX.  $\lceil \cdot \rceil$  denotes a ceil rounding operation. We choose this linear relationship instead of the actual expected physical propagation time, as this model basically allows to introduce

higher TO, whereas the level of TO can be adjusted at will by an appropriate coefficient, while we arbitrarily select  $1 \frac{\text{sym}}{\text{m}}$ . Hence, despite the limited dimensions of the investigated area, the principal robustness for an increased level of TO can be studied as it will be prevalent in an extended area. All nodes transmit with  $E_b = 1$  and the noise variance is  $\sigma_n^2 = 10^{-4}$ .

Fig. 6 depicts the outage rate with respect to  $N_{\text{nodes}}$  for varying  $N_{\text{paths}}$ . The advantage of cooperative transmission compared to classical non-cooperative multi-hop communication is on hand:  $R_{\text{out}}$  is significantly lower. According to the results of previous section, the benefits of multipath propagation are recognizable, too. For an increased number of paths, the frequency selectivity increases which the outer code can exploit, i. e. diversity over frequency is attained, leading to an overall increased performance. The proposed multi-carrier systems approximately achieves the same performance as the single-carrier system presented in [11] if the energy loss due to the cyclic prefix is considered, whereas a more detailed comparison between both is given in Section VI.

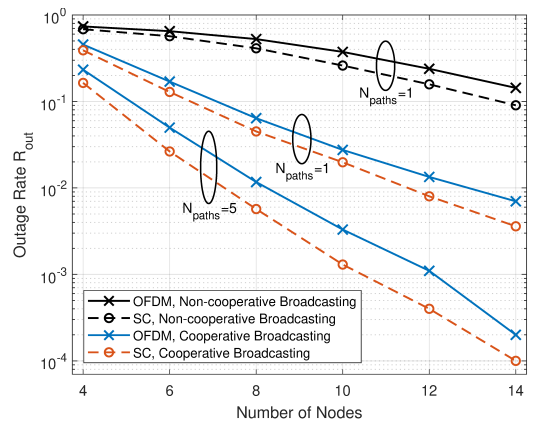


Fig. 6. Outage rate vs. population size

## VI. COMMENTS ON THE BENEFITS OF AN OFDM SYSTEM

In [11] we have proposed a comparable single-carrier system (QAM, time-domain equalization) that enables distributed cooperative communication in presence of the same impairments. Both systems are able to mitigate the impact of imperfections and basically attain the same diversity and outage performance. The single-carrier system has a slight advantage as the cyclic prefix and the usage of guard carriers, etc. causes an energy loss for the OFDM system, which is why accordingly a better BER vs.  $\frac{E_b}{N_0}$  as well as a lower  $R_{\text{out}}$  (see Fig. 6) can be achieved. Nonetheless, this is a structural disadvantage of an OFDM system, whereas the concrete impact is strongly related to the specific design. Without any cyclic prefix or respectively without considering this power loss, both schemes achieve the exact same performance. Thus, both are very well suited to establish distributed cooperative transmission for practical MANETs. The major contribution of this paper is to point out, that multiple carrier frequency offsets can be mitigated, so that there is no performance degradation. Hence, employing LSDCs to establish an efficient cooperative

transmission scheme is feasible for low-cost hardware.

At the end, the decision, which scheme is to be preferred, is closely related to the planned application, while both schemes have been compared to each other several times in previous research work. Fundamentally, both have the same potential [17]. If channel state information is available at the TX (CSIT) so that adaptive loading is possible, OFDM has a distinct performance advantage. Neglecting CSIT, OFDM typically offers a larger rate region in a multipoint to point communication than single-carrier systems [18], whereas it is shown that single-carrier schemes perform better in a slow-fading multipath channel [19]. One major disadvantage of OFDM is the peak-to-average power ratio (PAPR) that can be quite high and problematic if amplifiers with strong nonlinearities are used [20].

To sum up, our proposals utilize the fact that an iterative DFE receiver has to be already used due to the structure of LSDCs regardless of the channel model. On the one hand, the system from [11] allows a single-carrier scheme to effectively deal with strong multipath propagation which is actually a goodness that is ascribed to multi-carrier schemes. On the other hand, the system presented in this paper allows an OFDM system to effectively deal with multiple CFO. A problem, for which no sophisticated solution has been presented up to now (to the best of the authors' knowledge) and that has been considered a major drawback for the practical implementability. A single-carrier system might be better suited for low-complexity, battery-powered networks where each node has only limited computational power. In contrast, an OFDM system might be a wise choice for networks composed of more powerful nodes as multi-carrier schemes are in principal more flexible.

## VII. CONCLUSION

Within this paper we propose a communication system composed of adapted LSDCs in combination with an effective equalizer structure that allows to establish cooperative communication for distributed nodes in a MANET. The suggested system is tolerant against multiple timing and carrier frequency offsets. Differing to proposed comparable schemes, the latter can be several times higher than the subcarrier spacing without having a negative impact on the performance as long as the filtering bandwidth at the receiver is large enough. Additionally, the system requires reasonable computational effort. A scalable suboptimal iterative receiver within the proposed equalizer structure is sufficient to exploit a near optimum transmit diversity gain.

Upcoming variants of MANETs like VANETs and FANETs introduce high node mobility that typically leads to frequent disconnections and topology changes. As common routing protocols rely on broadcasting topology control messages, the overall scalability is limited [21]. Having demonstrated the benefits of our system in particular for cooperative broadcasting in MANETs, it can be stated that our proposals are very promising for an improvement of the overall scalability.

Acknowledgement: This research work has been funded by *armasuisse Science and Technology*.

## REFERENCES

- [1] A. Dusia and A. S. Sethi, "Software-defined architecture for infrastructure-less mobile ad hoc networks," in *2021 IFIP/IEEE Int. Symp. on Integrated Network Management (IM)*, pp. 742–747, 2021.
- [2] M. Yüksel, R. Rolny, M. Kuhn, and M. Kuhn, "Applicability of space-time block codes for distributed cooperative broadcasting in manets with high node mobility," *VTC Spring 2022 (to appear)*, 2022.
- [3] T. K. Bhatia, R. K. Ramachandran, R. Doss, and L. Pan, "A comprehensive review on the vehicular ad-hoc networks," in *2020 8th Int. Conf. on Reliability, Infocom Technologies and Optimization (Trends and Future Directions) (ICRITO)*, pp. 515–520, 2020.
- [4] J. Lin, W. Cai, S. Zhang, X. Fan, S. Guo, and J. Dai, "A survey of flying ad-hoc networks: Characteristics and challenges," in *2018 Eighth Int. Conf. on Instrumentation Meas., Computer, Comm. and Control (IMCCC)*, pp. 766–771, 2018.
- [5] H. Wang, Q. Yin, and X.-G. Xia, "Full diversity space-frequency codes for frequency asynchronous cooperative relay networks with linear receivers," *IEEE Trans. on Comm.*, vol. 59, no. 1, pp. 236–247, 2011.
- [6] Q. Huang, M. Ghogho, and J. Wei, "Data detection in cooperative stbc-ofdm systems with multiple frequency offsets," *IEEE Signal Processing Letters*, vol. 16, no. 7, pp. 600–603, 2009.
- [7] D. Veronesi and D. Goeckel, "Cth15-4: Multiple frequency offset compensation in cooperative wireless systems," in *IEEE Globecom 2006*, pp. 1–5, 2006.
- [8] X. Li, F. Ng, and T. Han, "Carrier frequency offset mitigation in asynchronous cooperative ofdm transmissions," *IEEE Trans. on Signal Processing*, vol. 56, no. 2, pp. 675–685, 2008.
- [9] F. Sánchez, T. Zemen, G. Matz, F. Kaltenberger, and N. Czink, "Cooperative space-time coded ofdm with timing errors and carrier frequency offsets," in *2011 IEEE Int. Conf. on Comm. (ICC)*, pp. 1–5, 2011.
- [10] A. Wittneben and M. Kuhn, "A new concatenated linear high rate space-time block code," in *VTC Spring*, vol. 1, pp. 289–293, 2002.
- [11] M. Yüksel, R. Rolny, M. Kuhn, and M. Kuhn, "Distributed cooperative transmission in manets with multiple timing and carrier frequency offsets," *PIMRC 2022 (to appear)*, 2022.
- [12] M. Kuhn, I. Hammerström, and A. Wittneben, "Linear scalable dispersion codes for frequency selective channels," in *Proc. of the 8th Int. OFDM-Workshop*, 2003.
- [13] V. Jodalén, B. Solberg, and S. Haavik, "Nato narrowband waveform (nbwf) - overview of link layer design," *FFI-rapport 2009/01894 (online available)*, 2011.
- [14] Y. Guo, G. Liu, I.-T. Lu, J. Ge, and H. Ding, "A new time and frequency synchronization scheme for ofdm-based cooperative systems," in *IEEE Long Island Systems, Applications and Technology (LISAT) Conf. 2014*, pp. 1–5, 2014.
- [15] E. Keramat, N. Kauffroath, K. Karbasi, H. Zhao, B. Daneshrad, and G. Pottie, "Experimental results for low overhead frequency offset estimation in manets with concurrent transmission," in *MILCOM 2017*, pp. 69–72, 2017.
- [16] M. Kuhn and A. Wittneben, "A new scalable decoder for linear space-time block codes with intersymbol interference," in *VTC Spring*, vol. 4, pp. 1795–1799, 2002.
- [17] R. Fischer and C. Stierstorfer, "Comparison of code design requirements for single- and multi-carrier transmission over frequency-selective mimo channel," in *Proceedings. Int. Symposium on Information Theory, 2005. ISIT 2005.*, pp. 1145–1149, 2005.
- [18] R. Fischer and C. Stierstorfer, "Single- and multicarrier transmission in multipoint-to-point scenarios with intersymbol interference: A comparison," in *4th Int. Symposium on Turbo Codes & Related Topics; 6th Int. ITG-Conference on Source and Channel Coding*, pp. 1–6, 2006.
- [19] D. Klovsky, S. Periyalwar, and S. Fleisher, "Comments on multi-carrier and single-carrier digital modulation in a multipath radio channel," in *Proceedings of Canadian Conf. on Electrical and Computer Eng.*, pp. 381–384 vol.1, 1993.
- [20] P. Franceschetti, V. Greco, G. Redaelli, and G. Coppola, "Analysis of single and multi carrier modulation schemes for 42 ghz broadband wireless systems," in *IEEE GLOBECOM 1998*, pp. 1924–1929 vol.4, 1998.
- [21] G. Kaur and P. Thakur, "Routing protocols in manet: An overview," in *2019 2nd Int. Conf. on Intelligent Computing, Instrumentation and Control Technologies (ICICT)*, vol. 1, pp. 935–941, 2019.